Energy & Buildings 282 (2023) 112809

Contents lists available at ScienceDirect

Energy & Buildings

journal homepage: www.elsevier.com/locate/enb

Effects of urban heat island mitigation strategies in an urban square: A numerical modelling and experimental investigation

Gabriele Battista [a,*], Emanuele de Lieto Vollaro [b], Paweł Ocłoń [c], Roberto de Lieto Vollaro [a]

[a] Roma TRE University, Department of Industrial, Electronic and Mechanical Engineering, Via Vito Volterra 62, 00146 Rome, Italy
[b] Roma TRE University, Department of Architecture, Largo Giovanni Battista Marzi 10, 00154 Rome, Italy
[c] Cracow University of Technology, Department of Energy,al. Jana Pawła II 37, 31-864 Krakow, Poland

ARTICLE INFO

Article history:
Received 17 November 2022
Revised 12 January 2023
Accepted 17 January 2023
Available online 20 January 2023

Keywords:
Overheating
Urban heat island
Mitigation strategies
ENVI_met
Model calibration
Experimental campaign

ABSTRACT

It is generally recognized that both urbanization and climate change contribute to the emergence of urban heat islands (UHI). Urban areas frequently encounter summertime local overheating, which is stressful and negatively affects a building's systems capacity to maintain the indoor air temperature set-point. UHI has sharply increased during the last 10 years as a result of shifting land use patterns, escalating urbanization, and declining plant and water supplies. The scientific community has recently paid a lot of attention to studies on UHI mitigation techniques, including those utilizing green roofs, cool materials, vegetation, and water supplies.

In this work, a square in Rome was experimentally and numerically investigated to assess a potential remedy for reducing outdoor air temperatures. A calibrated numerical model was made using the ENVI met tool, and several types of mitigation scenarios were looked at in order to lessen the area's warming and analyze the impacts of the recommended remedies on decreasing air temperature. The study's findings show that changing the pavement's albedo and adding more vegetation inside the square enhance the thermal conditions of the air. The use of grass pavers, in particular, would provide the biggest advantages.

1. Introduction

Urban heat islands are mostly caused by urbanization and climate change. When compared to the rural population, the urban population is growing. Deforestation and soil consumption are also connected to urbanization. By dividing the population of urban areas by that of rural areas, the urbanization rate may be calculated. Urban growth refers to a rise in the population rather than an extension of the surrounding area [1].

All around the world, people made the transition from the countryside to the metropolis, although not always in the same way [2]. From 2 to 3 % at the beginning of the nineteenth century to 30 % in the middle, growth has accelerated in recent centuries. It didn't stop until 2017 when the urban population surpassed the rural one [3].

The urban heat island phenomenon is a result of urban expansion [4,5]. An urban microclimate phenomenon is known as urban heat island [6]. It was initially described by Luke Howard in his 1818 paper "The Climate of London" [7] as the rise in temperatures in urban regions relative to what occurred in rural areas. When wind fluxes are decreased, this phenomenon is more prevalent. The high solar radiation absorption on concrete and asphalt, which releases the heat of the day during the night [8,9], the reduction of green spaces and naturally permeable surfaces, thermal human sources related to transportation and air conditioning systems, low soil water retention, and low levels of evaporation are just a few of the causes of the temperature difference between cities and rural areas, which can range from 0.5 to 3 °C.

The consequences of urban heat island can have a negative influence on people's life. [10,11]. This disease is directly tied to the quality of the air and water. Additionally, it increases air conditioning system usage because buildings cool down more often [12,13], which increases power consumption [14,15] and increases pollutant emissions in metropolitan areas [16,17].

Due to shifting land uses, growing urbanization, and a decline in plants and water supplies during the past 10 years, UHI has significantly increased [18–20]. Urban growth in Shanghai has disrupted the surface energy balance and increased the sensible heat flow, according to Zhang et al. [21]. This is because there are less plants and water bodies, which reduces the difference between the land surface temperature (LST) of the city and the urban perimeter.

* Corresponding author.
E-mail address: gabriele.battista@uniroma3.it (G. Battista).

https://doi.org/10.1016/j.enbuild.2023.112809
0378-7788/

LST values in Delhi's commercial and industrial zones were 4 °C higher than in the suburbs, according to Mallick et al. [22]. This is caused by both human activity and changes in plant density.

Climate conditions and urban heat island have a strong relationship that has a big influence on energy usage. Hwang et al. [23] report that an urban heat island intensity level between 1.9 °C and 3.2 °C caused Taiwan to experience an increase in household yearly cooling energy from 1979 to 2003 of 87.3 % to 243.6 %. According to the calculations, the future UHI will be 5.8 °C with a maximum yearly cooling energy gain of 476.9 %. In a case study in the Yangtze River Delta, Du et al. [24] found that there is no correlation between population density and urban heat island intensity in metropolitan regions. However, there is a positive association between UHI intensity and the urban area and energy use. The average wind or rainfall rate and the severity of the UHI did not correlate well [25–28].

Boulevard Street and high-rise residential structures in Putrajaya, Malaysia, have 4 °C lower temperatures than low-rise ones, according to research by Qaid et al. [29]. The temperature is 1 °C lower in the low-rise buildings than it is in the nearby suburban areas. Low-rise buildings experience thermal stress for a longer period of time than high-rise residential structures and boulevard roadways. In the Mendoza metropolitan area of Argentina, a tiny non-forest canyon appears to have the warmest area, whereas a multi-azimuthal neighbourhood grid appears to have the coolest air temperature, according to Sosa et al. [30]. The combined effects of neighbourhood grid and urban canyon plan were also found to have a substantial influence on urban heat island reduction. According to Li et al. [31], the link between near-surface urban pollution island and atmospheric urban heat island is −0.31 and is most prominent at night. According to the study, clear nights cause an increase in the surface urban heat island of 12 %.

Recent times have seen a lot of interest in studies on UHI mitigation techniques, including those utilizing green roofs [32,33], cool materials [34], vegetation [35,36], and water sources [37,38]. For both big urban areas, such as cities as a whole, and smaller localized urban areas, such as urban canyons, adopting mitigation strategies is essential [39,40]. Matias and Lopes [41] investigated how the radiation balance of urban materials impacts the air temperature in an urban canyon.

Larger studies showed that the increasing adoption of cool and green roof technologies has a profound impact on urban heat island reduction. According to Georgakis et al. [42], a 7–8 °C drop in surface temperature may be achieved by lowering wall surfaces by 2–3 °C and increasing the albedo value of pavements at ground level. The overall air temperatures in the urban street canyon dropped by 1 °C, according to the research. Peron et al. [43] found that the temperature decreased by roughly 4 °C when cool materials and green permeable surfaces were utilized in place of the old pavements and roofs in a section of Mestre, Venice. Pavement has an impact on UHI effects as well [44,45].

Numerous studies and conclusions that have been published in the literature [46–48] discuss the effects of UHI on Rome's climatic conditions and the influence of mitigation strategies, particularly in terms of decreasing air temperature values in certain metropolitan regions. Zinzi et al. [47] 's research of the impacts of heat waves on three Rome neighbourhoods from 2015 to 2017 found that the UHI index might increase by up to 1.5 °C as a result, despite an 87 % increase in cooling energy usage in buildings during these times. Rome's UHI has values of 0.7 °C and 1.0 °C, respectively, and is more severe in the summer than it is in the winter, according to a review of data spanning three years from 2015 to 2017 [48]. Battista et al. [49] examined a densely populated Roman square to ascertain the impact of various UHI mitigation techniques on air temperatures and outdoor thermal comfort conditions. Salata et al. [50] carried out a field survey investigation in Rome to evaluate outdoor spaces that are crucial for minimizing the effects of UHI. Using monitoring data and numerical analysis, another study evaluated different UHI mitigation strategies in Rome. The results showed that while using reflective materials and vegetation could lower the temperature by up to 2 °C, new urban development could increase the average ambient temperature by up to 3.5 °C during the midday [51]. Salata et al. [52] 's computer model of a university campus in Rome may be used to evaluate different UHI mitigation strategies. In Rome's localized urban districts, highly reflective materials [53], green roofs [54] and urban vegetation [55] are typical strategies. The urban characteristics of a historic city like Rome, such as its winding streets that form urban canyons and its traditional roof materials composed of low solar reflectance Roman clay tiles, may have an impact on the UHI index [56,57].

This project's goal is to assess several technical options for improving the microclimate in a densely populated area of Rome, specifically Mancini Square (Italy). A numerical model was created using the ENVI_met program in order to assess the impact of the mitigation options in terms of a decrease in air temperature [58]. Data on the relative humidity and air temperature were gathered in order to set the boundary conditions and calibrate the numerical model.

2. Materials and methods

2.1. Methodology

The examination of the chosen region is the basis of this study, which aims to assess the efficacy of various mitigation strategies for the impacts of urban heat islands. The stages that make up the applicable approach are indicated in Fig. 1 and are as follows:

1. Individuation on a heavily populated metropolitan region with minimal green spaces;
2. Selection of the more successful methods able to reduce the outdoor air temperature of the urban area;
3. Experimental monitoring, taking into consideration the structures' shape, albedo, and the surrounding environment's temperature, rainfall, relative humidity, solar radiation, and wind speed;
4. Numerical modelling generation and calibration using ENVI_met;
5. Analysis of mitigation strategies using numerical simulation with a comparison of improvement scenario and actual urban area situation. Comparisons were analysed through the air temperature spatial variation during the hour of 6am, 1 pm and 6 pm, and analysis on the air temperature variation during the whole day of simulation were performed into three different points: one very close to the objected retrofit area; the secondo is related to a point in the middle of the retrofit area; a last one placed in an area far from the requalified site.

2.2. Case study

This work uses Mancini Square in Rome as its case study. Rome shows a Mediterranean climate with temperate winter and hot summer, with temperatures ranging from 0 to 36. Rome has 1415 degree-days that represent the sum of the days of a conventional annual heating period (from 1st November to 15th April), considering the days with a positive difference between the indoor air temperature fixed at 20 °C and the outdoor one.

The study area is made up of broad asphalt zones that are used as walkways and pavement. Additionally, the examined Mancini Square contains low trees that don't offer enough shade. The effi-

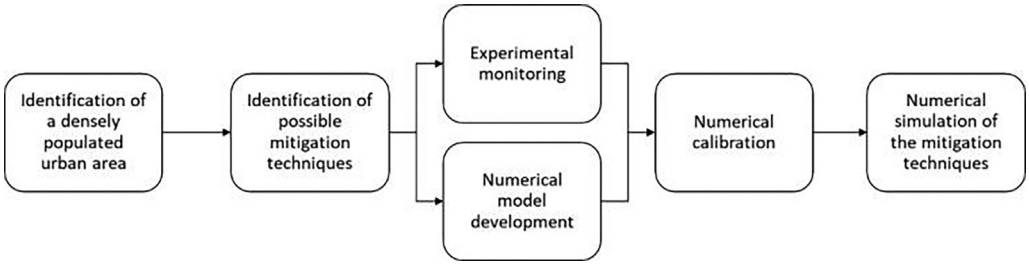

Fig. 1. Flowchart of the methodology.

cacy of the mitigating measures is amplified in this area due to the high population density. Fig. 3a shows an aerial view of the Flaminio district simulated area as well as the Mancini and Carracci squares and the position of the weather station that recorded the air's temperature and relative humidity. This area is close to both the Tiber River and the center of Rome. Mancini Square is situated in latitude 41°55′51.1″N and longitude 12°27′51.9″E and has a surface area of approximately 6000 m^2. Between the city's centre and its northern edge is where the study area is situated. In specifically, the analysed region is 4.6 km from the city centre and 6 km from the city's edge.

The Flaminio district is made up of intensive construction buildings and small buildings. The area was built starting from 1909 with industrial settlements and public buildings. During the war years, the military barracks complex was wedged into this area. The first residential buildings were built after the end of the Second World War. Mainly the buildings have characteristics typical of the construction typologies of the 1950 s. In particular, the buildings built on Viale Pinturicchio which runs alongside Mancini Square were built around 1960 [59]. The typical stratigraphy covering the construction period of 1900–1950 is characterized by bricks plastered on both sides with a total thickness of 0.60 m [60].

2.3. Mitigation strategies

The best practices used in other case studies in the literature were followed when choosing the mitigation techniques, however those that could not be used due to urban limits were not taken into consideration. The following are the ones chosen for this study:

1. The use of cool pavements with high albedo and permeability values, with an albedo of 0.50;
2. The use of grass pavers rather than conventional asphalt;
3. The expansion of vegetation with species comparable to those currently present;
4. The addition of a projecting roof for shade in Mancini Square.

In reality, there are frequently more pavements than green spaces in cities, and asphalt in particular is one of the key contributors to the rise of the urban heat island. Given that the reflecting performance is better than that of the commonly used asphalt, asphalts with high albedo led to a lighting savings at night.

Because cool pavements have superior reflecting and permeability qualities than conventional asphalt, they can be utilized to lower the pavement's solar absorption. Grass pavers can be used as cool materials despite the traditional mitigation technique of using ordinary cool pavements. The permeability and evapotranspiration effects of these porous pavements, which are constructed of cool, solar-reflective materials blocks with an alternate layer of grass, are increased.

The shading projecting roof can reduces the amount of solar radiation absorbed by the asphalt with a consequent reduction of the air temperature near the intervention.

Among the aforementioned mitigating strategies, "water mirrors" include placing water sources inside the square to enhance the cooling effects brought on by water evaporation. Additionally, the existence of these water reflectors reduces the overall quantity of solar energy that Mancini Square's asphalt absorbs.

2.4. Experimental campaign

Two weather stations were put in at Carracci Square and Mancini Square to get the most accurate model (see Fig. 2). The data collected by the weather station installed at Mancini Square served as the calibration data for the numerical model.

A pluviometer, anemometer, temperature, humidity, and other weather sensors are all included in the Davis Vantage Vue weather station. Main characteristics of the sensors are:

- Rain rate with resolution of 0.01″ per tip or 0.01 mm with a range from 0 to 30″/h (0 to 762 mm/h) and an accuracy of ±5 % under 10″/h;
- Wind speed resolution 0.5 m/s with a range from 0 to 89 m/s and an accuracy of ±1 m/s or ±5 % whichever is greater;
- Wind direction resolution of 1° with a range from 1 to 360° and an accuracy of ±3°;
- Inside air temperature resolution of 0.1 °C with a range from 0 °C to 60 °C and an accuracy of ±0.3 °C;
- Outside air temperature resolution of 0.1 °C with a range from −40 °C to 65 °C and an accuracy of ±0.5 °C above −7°C and ±1 °C under −7°C;
- Humidity resolution of 1 % with a range from 1 to 100 % and an accuracy of ±2 %.

The portable Spechtrophotometer CM-2600d Konica Minolta was utilized for the experimental study of pavement and wall surfaces. Measurements were carried out to analyse the various behaviours of the materials while taking into consideration various colour combinations and roughness values. Main characteristics of the instrument are:

- Diffused illumination at 8-degree viewing angle;
- Integrating sphere diameter of 52 mm;
- Wavelength range from 360 nm to 740 nm;
- Wavelength pitch 10 nm;
- Reflectance range from 0 to 175 %;
- Resolution of 0.01 %.

In 2021, the weather stations were put in place. To gather data under various weather circumstances, data were specifically collected from July 21 to August 2. It was possible to observe that the weather station in Carracci Square is less exposed to the sun that the one in Mancini Square, and one day during which the data

(a) (b)

Fig. 2. Installation of the weather stations at Carracci Square (a) and Mancini Square (b).

are similar will be chosen for the calibration of the numerical model.

2.5. Numerical model setup

The numerical model was made using the ENVI_met tool version 4, which is based on the SVAT model (Soil, Vegetation and Atmosphere Transfer). With the help of this application, it is possible to simulate the microclimate of an urban area while accounting for all soil, atmospheric, and integration-related activities as well as those related to surfaces, vegetation, water features, and pollution sources. Fig. 3b displays the geometrical features and the accompanying numerical model.

The numerical simulations were run for a total of 30 h, beginning at 6p.m. on July 21, 2021, and finishing at 12 a.m. on July 22, 2021. The findings are relevant to July 22, 2021, when greater air temperatures were noted. Experimental data from Carracci square were used as the forced air temperature and humidity to the boundary of the numerical model due to its position on the numerical domain boundary. Average wind speed and wind direction of the day in Carracci weather station were used in the model.

A quadrilateral grid imposed by ENVI met discretizes the domain. Due to the domain's size (a square area of 624 m on each side), it was important to strike a compromise between the simulation's quality and the turnaround time for the results [35,49]. The

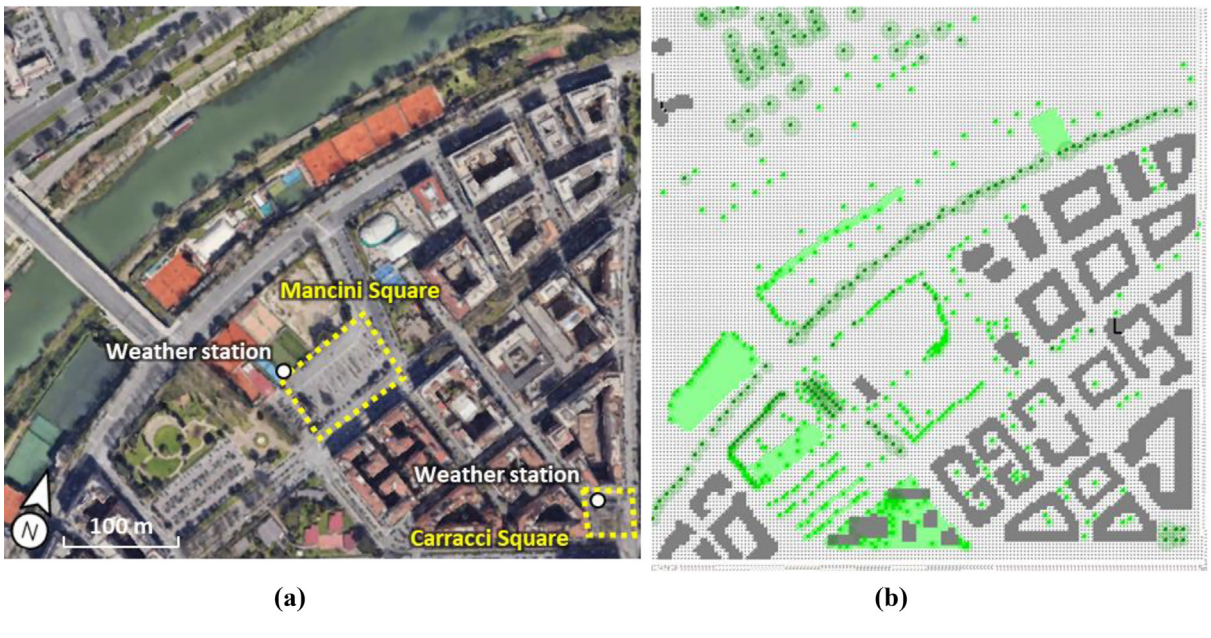

(a) (b)

Fig. 3. Comparison between the aerial view a) and the ENVI_met model b) of the simulated domain. ENVI_met. Positions of the weather stations and the Mancini and Carracci squares are shown.

grid has 156(x) × 156(y) × 30(z) cells, a grid size of 4 m, and a discretization of time of 10 s.

Buildings are located near to the created model's limits, thus its grid points cannot respond to outside forces the same way they do inside the model. This calls for the addition of 5 nested grids to the model.

Several atmospheric quantities are needed to run the numerical model in ENVI-met. The input values used in this study are reported in Table 1.

3. Results and discussions

3.1. Experimental results

The experimental campaign was done during the period from 21st July to 3rd August 2021 monitoring the microclimatic conditions such as air temperature and relative humidity. The results are shown in Figs. 4 and 5.

As shown in the trend measurement of Figs. 4 and 5, it is evident the heat waves happened in that period. In fact, considering the data from Mancini square weather station (see Fig. 3a), the air temperature data rise from a minimum of 19.9 °C recorded during the early hours of the day (about 5 am) up to a maximum of 39.3 °C recorded during the hottest hours of the day (about 1 pm). During the experimental campaign the average air temperature was 29.0 °C.

Regarding Carracci square weather station (see Fig. 3a), the air temperature recorded was from 21.1 °C to 37.7 °C with an average value of 29.2 °C. It is possible to notice that there is a warmer condition inside the Mancini square that justify its choice as the case study for the present paper. Data from Carracci square were used as the forced air temperature to the boundary of the numerical model.

About the relative humidity, it was possible to notice that values recorded vary from 17 % to 93 % with an average value of 53.5 % for Mancini square, while values are from 17 % to 89 % with an average value of 51.6 % for Carracci square. The variability of the relative humidity is very stressed due to the proximity of the Tiber River. These values bring to the attention that there is the possibility to have different thermal comfort conditions that need to be investigated in order to choose the appropriate mitigation techniques that can reduce the air temperature and control the relative humidity in order to bring a better thermal comfort situation.

3.2. Numerical model calibration

Calibrating the findings is the first stage in the numerical model implementation process. In particular, comparisons were made between the simulated and actual air temperatures and relative humidity.

Table 1
Input parameters in the numerical analysis.

Parameter	Value
Air temperature at 2 m (K)	forced
Relative humidity at 2 m (%)	forced
Daily average wind speed (m/s)	1.26
Daily average wind direction (°)	35 (North-East)
Specific humidity at 2500 m ($g_{water\ vapor}/kg_{air}$)	7
Roughness length at measurement site (m)	0.01
Albedo of building walls and roofs (–)	Range from 0.30 to 0.89
Albedo of soil (–)	0.38
Albedo of pavements (–)	0.11
Start simulation at day	21/07/2021
Start simulation at time	6 pm
Total simulation time in hours (h)	30

The calibration process is assessing the relative inaccuracy of simulated and measured data where the weather station of Mancini Square was installed, simulation after simulation. The numerical model's input variables for the air temperature and relative humidity were meticulously revised for each simulation in order to reduce this mistake. In particular, the calibration consists of checking, simulation after simulation, the relative error of simulated and measured data where the weather station was installed. In each simulation, to minimize this error, it was corrected point by point the forced input data of the numerical model related to the air temperature and relative humidity.

Two statistical indices were used to evaluate the variation between the experimental and simulated data. The quantitative indicators [51] used in this work are, taking into account the model-predicted P_j and observed variables O_j at each instant j, and the amount of examined data N_D, respectively:

- The Mean Bias Error (MBE) reveals if the model values are more than or lower than the actual data. This indicator does not work well when predicted values are alternately exceeded and underestimated since they set off against one another.

$$MBE = \frac{\sum_{j=1}^{N_D}(P_j - O_j)}{N_D} \quad (1)$$

- Mean Absolute Error (MAE), which accounts for the absolute difference between predicted and actual data, is comparable to the MBE indicator. Therefore, when the anticipated values fluctuate between being overestimated and underestimated, this indicator is useful.

$$MAE = \frac{\sum_{j=1}^{N_D}|P_j - O_j|}{N_D} \quad (2)$$

The MBE and MAE errors were calculated regarding the air temperature for each simulation, as a consequence of the iterative calibration technique mentioned above. A MAE value of 0.29 with a standard deviation of 0.39 and an MBE value of 0.06 with a standard deviation of 0.26 were obtained by the calibrated model. The deviation between the simulated and the measured data range from −0.45 to 0.98 °C, that correspond to a percentage deviation from −1.83 % to 3.44 % with a mean value of 0.14 %.

3.3. Numerical models of mitigation strategies

Numerical simulations were run in order to combine compatible mitigation strategies and create the most effective heat island mitigation scenario in order to assess the efficacy of urban heat island mitigation measures.

Particularly, a variety of mitigating techniques were used inside Mancini Square (see Fig. 3a) and configurations are shown in Fig. 6.

The analysed original scenario without any mitigation techniques is named Scenario 1. In this case wide asphalt zones are employed as sidewalks and pavement. Additionally, there are low trees that do not provide enough shade inside Mancini Square. Furthermore, in the proximity of the square there is an high traffic road and two parking area characterized by few trees.

Scenario 2 is related to the introduction of cool materials inside the square. In particular, it was used a cool pavement with an albedo equal to 0.5. As shown in Fig. 6, the intervention area is highlighted with the dotted red line and correspond to the whole square.

The adoption of a grass pavers as the pavement of the square is related to the Scenario 3. This case has the same configuration of

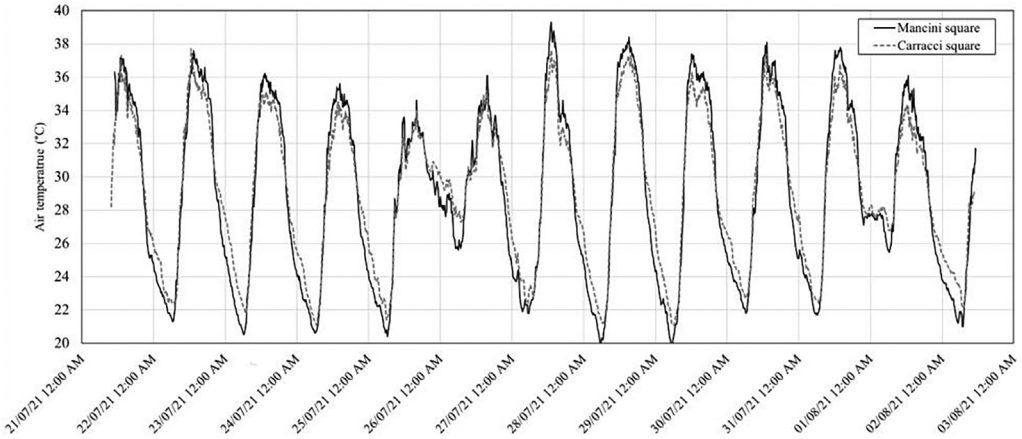

Fig. 4. Air temperature trend during the measurement campaign between 21st July to 3rd August 2021.

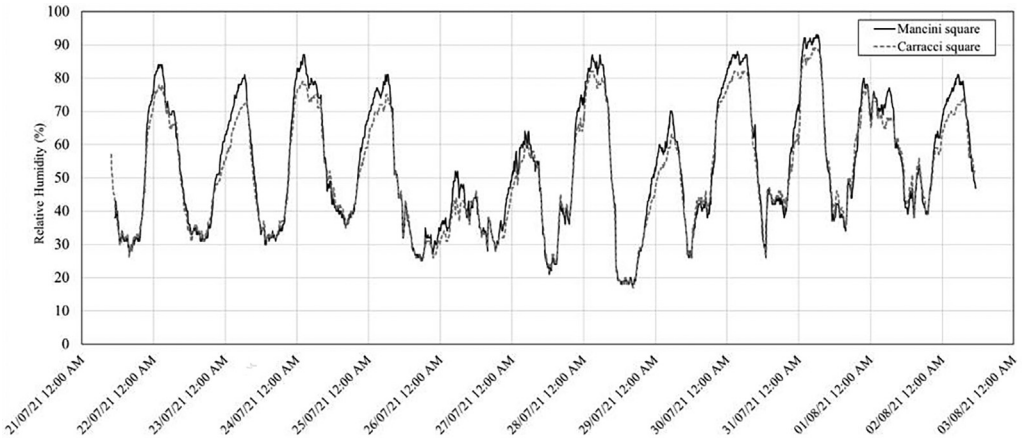

Fig. 5. Relative humidity trend during the measurement campaign between 21st July to 3rd August 2021.

the standard Scenario 1 with only the use of different type of pavements.

The improvement of the vegetation is considered in the Scenario 4. In particular, medium and tall trees and grass have been added in the centre of the square. Furthermore, it was improved the amount of trees in the park adjacent to the square as shown inside the red dotted line of Fig. 6.

Finally, in Scenario 5 a shading projecting roof was used as a mitigation techniques, as shown in Fig. 6. This case has the same configuration of the standard Scenario 1 with only the introduction of a shading projecting roof in the centre of the square.

3.4. Air temperature spatial variation

The air temperature spatial variations are shown in Fig. 7 at 6 am, 1 pm and 6 pm at 1.75 m above the ground, which is about where people usually stand. As a matter of fact, Cacciari et al. [61,62] finds in 2004 that the mean body height of Italian people is 1.776 m that near the value of 1.75 chosen in the present work due to the vertical discretization of the numerical model. Fig. 7 shows the outcomes of the mitigation plan strategies used in scenarios 2, 3, 4, and 5, which are all connected to scenario 1 and depict the area's real circumstances.

Taking into account the outcomes at the Mancini Square's centre, in Table 2 are shown the results for the different scenario. Considering the maximum air temperature decrease, a 0.88 °C drop is achieved by using cool material at 1 pm. When a grass paver is used, this decrease can reach 2.11 °C at 1 pm. This is a result of the benefits of mixing the cool pavement block material with the evapotranspiration impact of the grass.

The Scenario 4 vegetation improvement results in a 0.82 °C maximum drop in air temperature at 6 pm. This value is lower than the installation of grass pavers in Scenario 3 (when vegetation like grass is used), as the vegetation in Scenario 4 is only present in the centre of the square, as opposed to Scenario 3, where the entire square is subject to the mitigation method.

The square's projecting shade roof can reduce air temperature by up to 1.61 °C at 1 pm, but it's important to note that this benefit is limited to the space directly beneath the roof. Due to the original asphalt's poor reflectivity, the air temperature outside this region is greater.

It is possible to notice that there is a maximum air temperature decrease in the wormer hour of the day, while for the improvement vegetation scenario the maximum effect is during the afternoon. Furthermore, results in Table 2 shows that with the vegetation is possible to have a more constant air temperature decrease despite the other scenarios that have picks during the hottest hour of the day.

3.5. Time variation of air temperature

The effects of the various mitigation strategies were examined by comparing the estimated data in the three different locations in the simulation domain shown in Fig. 8a.

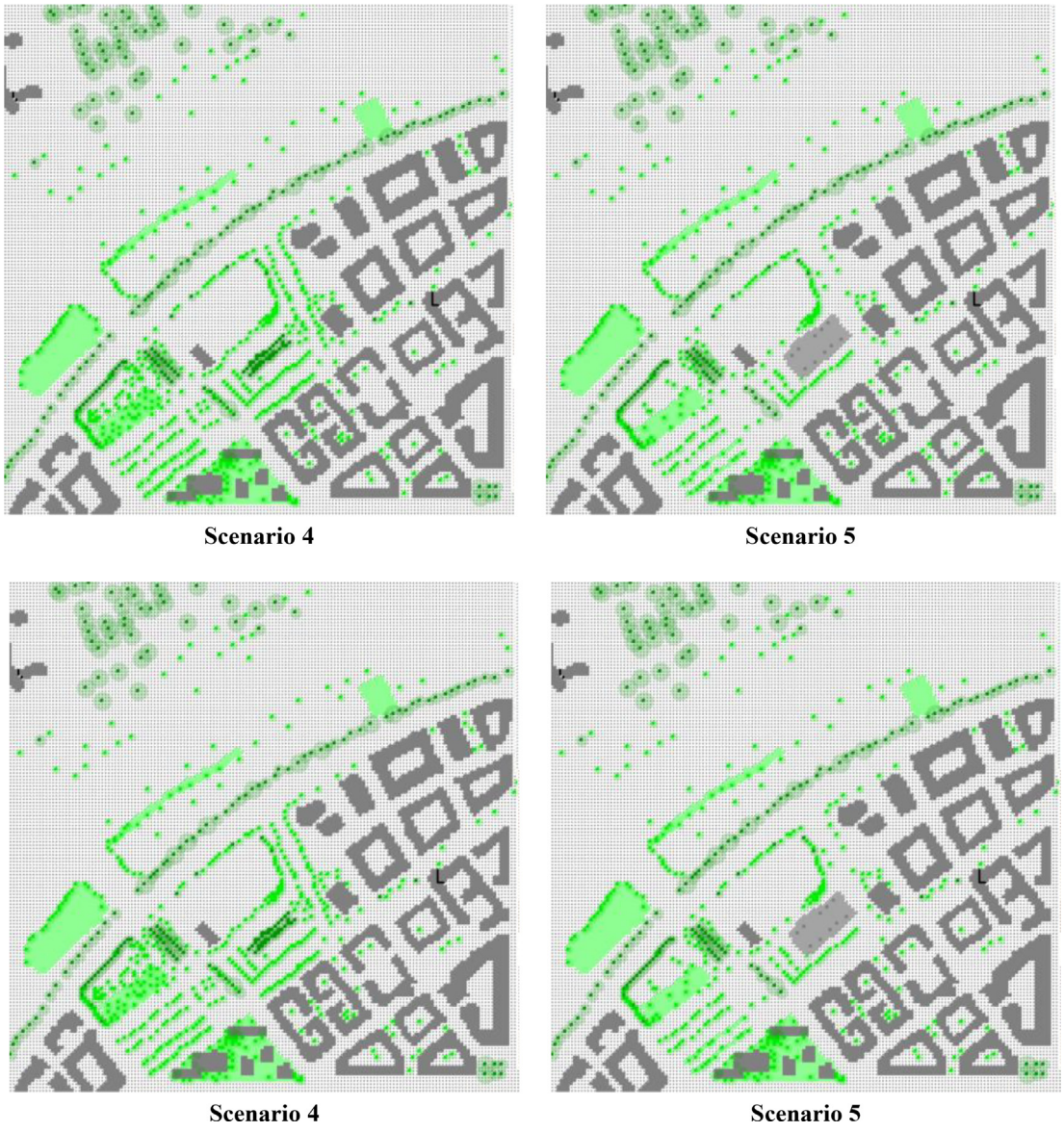

Fig. 6. Numerical model used for the mitigation scenarios.

The air temperature variations determined in three places (designated receptors R1, R2, and R3) at a height of 1.75 m above the ground are displayed in Fig. 8b, c, and d during various hours of the day. The receptor R1 is located very near to Mancini Square, the receptor R2 is connected to a location in the centre of the square, and the receptor R3 is located distant from Mancini Square's requalified area in the street that borders the square.

One can see that the impacts of the various mitigation strategies are minimal outside of the square. In fact, the whole trend in Fig. 8d, which relates to the *R*3 receptor, exhibits a temperature differential that is almost nil in comparison to the initial situation (Scenario 1).

It is feasible to corroborate the findings previously covered in paragraph 3.2 by taking into account the addition of a shade projecting roof in the square's centre. In fact, when comparing the findings at points R1 and R2 (see Fig. 8b and c), it is only at point R2, where the point is located at the same location as the installation of the projecting roof, that the trend is consistently negative throughout the day.

It has been established that the mitigation scenario including grass pavers results in a greater drop in air temperature with more benefits than the usage of cool materials. Additionally, the R2 location has more favourable impacts than the R1 location since the centre of the square has a higher concentration of asphalt components than the area considered for receptor R1.

It is possible to perceive a more significant drop in air temperature close to the enhanced vegetation area due to the medium and tall trees and grass planted in the centre of the square. However, as evidenced by the results of receptor R1, the addition of flora inside the square can lower the air temperature close by. Due to the replacement of an asphalt part of the square with vegetation, the air temperature differential in R1 also has a negative value at all times of the day.

The use of grass pavers in Scenario 3 (−1.35 °C), the use of a shading projecting roof in Scenario 5 (−0.85 °C), the improvement of vegetation in Scenario 4 (−0.60 °C), and the installation of cool materials in Scenario 2 (−0.39 °C) are the more effective techniques, according to results in the middle of the square (data from receptor R2 of Fig. 8c).

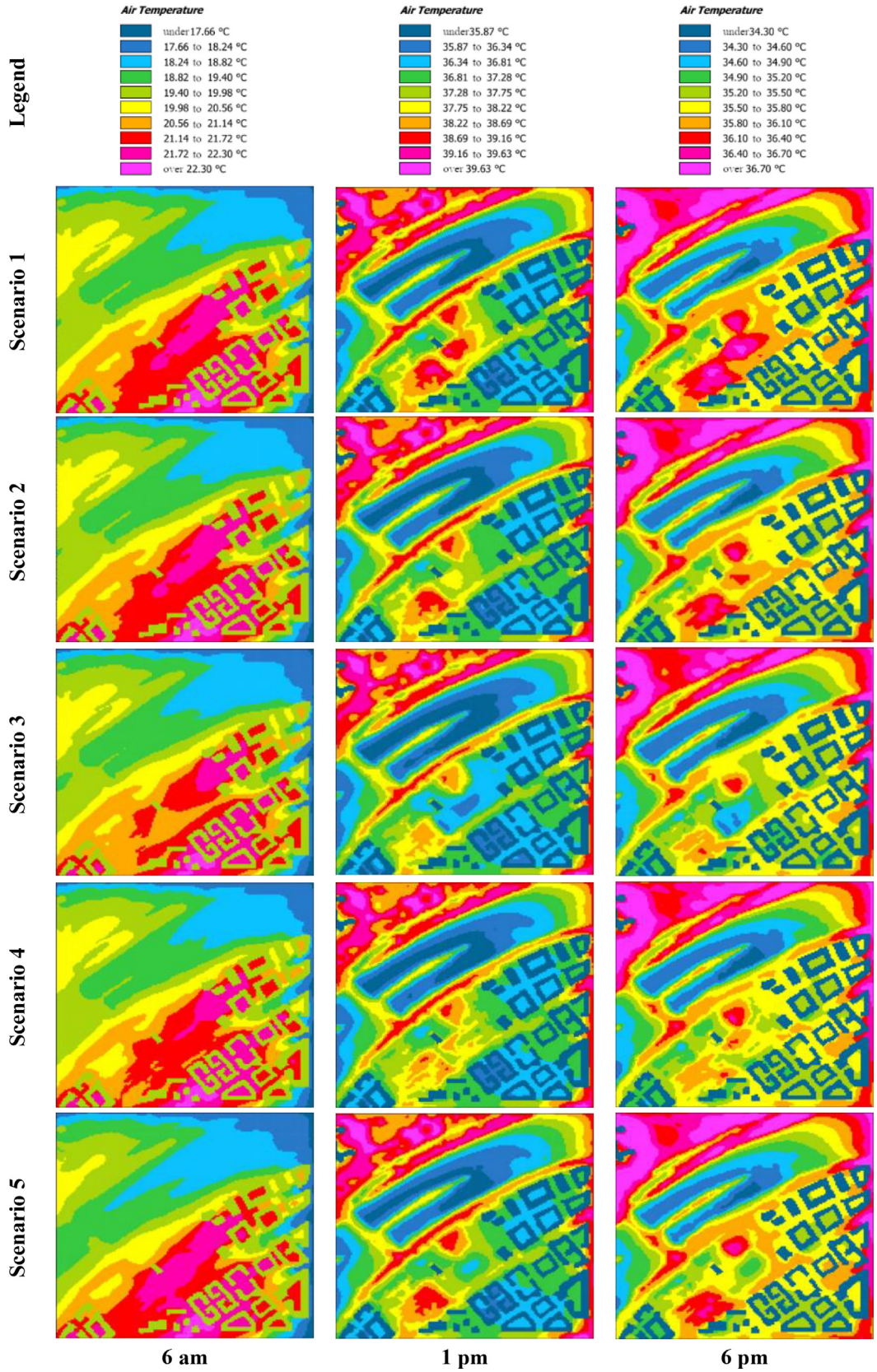

Fig. 7. Scenarios 1, 2, 3, 4 and 5: simulation of air temperature at 6am, 1 pm and 6 pm at an altitude of 1.75 m.

Table 2
Air temperature difference from standard case (Scenario 1) and the mitigation technique adopted at the Mancini Square's centre.

Time	Scenario 2	Scenario 3	Scenario 4	Scenario 5
6 am	−0.01	−0.57	−0.25	−0.05
1 pm	−0.88	−2.11	−0.72	−1.61
6 pm	−0.44	−1.52	−0.82	−1.42

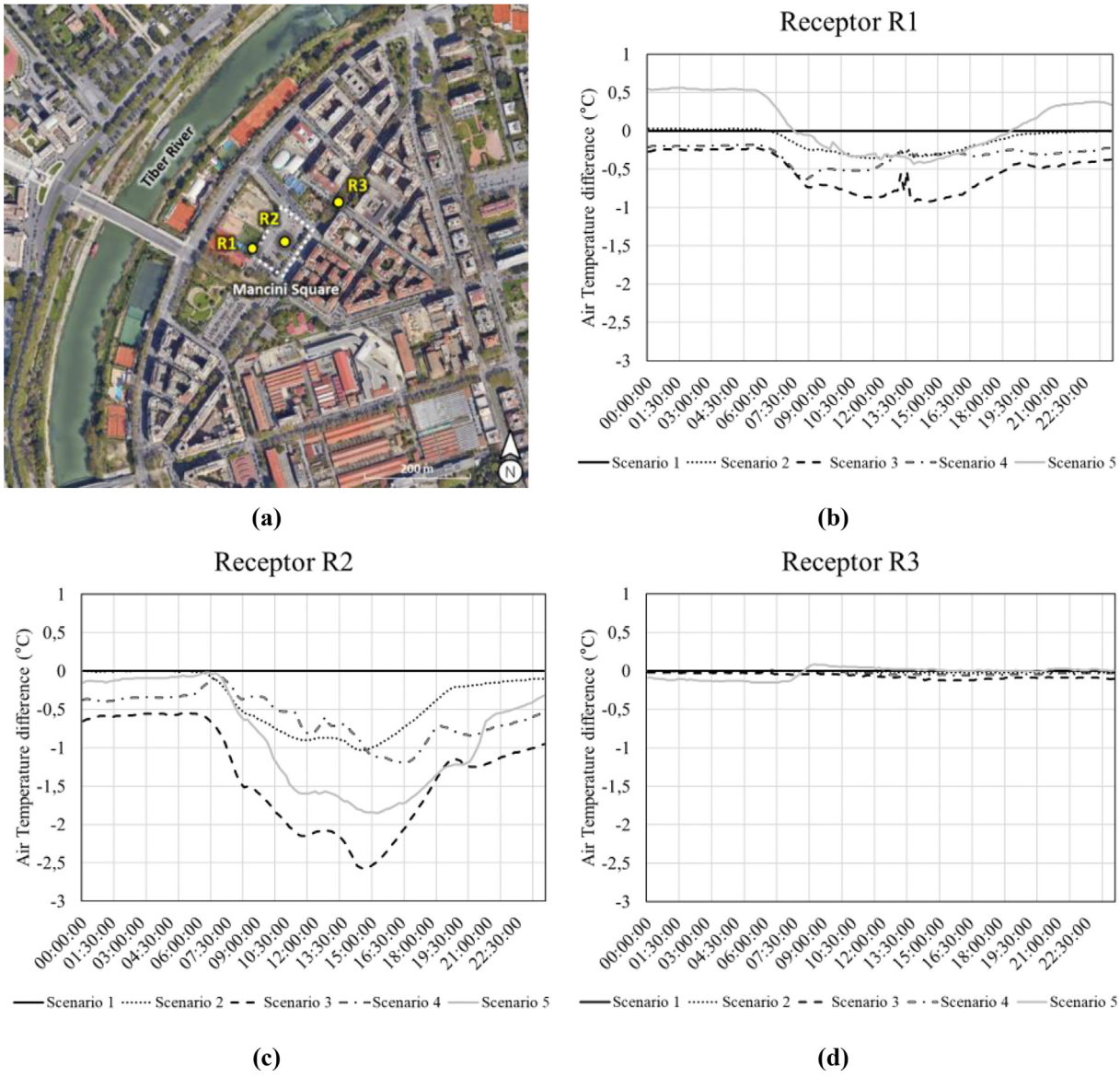

Fig. 8. Comparison of the Scenarios 2, 3, 4, 5 and the actual situation (Scenario 1) in terms of air temperature difference at an altitude of 1.75 m considering Scenario 1 as reference. The points of evaluation are shown in (a) while results are shown in (b), (c) and (d).

4. Conclusions

Numerous studies were conducted in many regions, including Italy, to evaluate urban overheating and appropriate mitigating measures. In this study, the focus was on an area inside Rome that is distinguished by a high density. Preliminary measurements in the chosen zone to be utilised for calibrated simulation were carried out in recognition of the limits of software in modelling complex objects as cities or parts of them. Additionally, measurements made on-site allowed for the determination of the albedo of the built materials, as well as the features of the current vegetation and the climatic conditions during the hottest period of the year.

In this study, many technical methods for improving the microclimate in a densely populated Roman neighbourhood were looked at. A numerical model was created using the ENVI met tool to assess the impact of the mitigation options in terms of a decrease in air temperature. Experimental data on the air temperature and relative humidity were gathered to set the boundary conditions and calibrate the numerical model.

After examining the outcomes of the treatments, it has been shown that altering the pavement's albedo means improving the

circumstances related to thermal stress, with the use of grass pavers proving to be the most advantageous. Additionally, the increased vegetation inside Mancini Square may result in a decrease in air temperature throughout the day for both regions inside and relatively adjacent to the square.

The climatic conditions are significantly locally impacted by the shade canopy, albeit this impact lessens as individuals move out of the shadows.

With interventions that may lower the air temperature up to 2.5 °C in the centre of the square and up to 1 °C in places that are very close to the square, the chosen heat island mitigation approaches make it feasible to lower the air temperatures at street level during the warmest part of the day.

Thus, the study offers insight into possible mitigation in a highly populated metropolitan area in the Mediterranean while also demonstrating that objectives and priorities must be clearly defined so that the best mitigation strategies may be used for the particular project. Future development of the present study is to analyse the effects of the mitigation strategies on the outdoor thermal comfort conditions.

CRediT authorship contribution statement

Gabriele Battista: Conceptualization, Methodology, Software, Resources, Investigation, Formal analysis, Writing – original draft, Writing – review & editing. **Emanuele de Lieto Vollaro:** Conceptualization, Data curation, Writing – original draft. **Paweł Ocłoń:** Visualization, Investigation, Supervision. **Roberto de Lieto Vollaro:** Visualization, Investigation, Supervision.

Data availability

No data was used for the research described in the article.

Declaration of Competing Interest

The authors declare that they have no known competing financial interests or personal relationships that could have appeared to influence the work reported in this paper.

Acknowledgments

The authors would like to thank the contribution of the Department of Architecture of the University of Roma Tre team headed by Prof. Paolo Desideri in which there was the participation of Francesca Romana Cattaneo, Roberto D'Autilia, Giorgia De Pasquale, Alessandro Gabbianelli, Luca Montuori, Enrico Nigris, Maria Pone and Matteo Staltari. The Department of Architecture of the University of Roma Tre team has done a collaboration to the project development with the Department of Industrial, Electronic and Mechanical Engineering research team headed by Prof. Roberto De Lieto Vollaro in which there was the participation of Gabriele Battista, Emanuele De Lieto Vollaro and Marco Formiconi.

References

[1] Urbanization over the past 500 years, 1500 to 2016, (n.d.). https://ourworldindata.org/grapher/urbanization-last-500-years?country=IND~CHN~OWID_WRL~USA~JPN (accessed October 30, 2022).
[2] M. Pesaresi, M. Melchiorri, A. Siragusa, T. Kemper, Atlas of the Human Planet - Mapping Human Presence on Earth with the Global Human Settlement Layer, (n.d.). https://doi.org/10.2788/582834.
[3] Number of people living in urban and rural areas, (n.d.). https://ourworldindata.org/grapher/urban-and-rural-population (accessed October 30, 2022).
[4] N.S. Mohammad Harmay, D. Kim, M. Choi, Urban Heat Island associated with Land Use/Land Cover and climate variations in Melbourne, Australia, Sustain. Cities Soc. 69 (2021), https://doi.org/10.1016/J.SCS.2021.102861.
[5] A. Vallati, L. Mauri, C. Colucci, Impact of shortwave multiple reflections in an urban street canyon on building thermal energy demands, Energ. Buildings 174 (2018) 77–84, https://doi.org/10.1016/J.ENBUILD.2018.06.037.
[6] R.A. Memon, D.Y.C. Leung, C.-H. Liu, An investigation of urban heat island intensity (UHII) as an indicator of urban heating, Atmos. Res. 94 (3) (2009) 491–500.
[7] L. Howard, The Climate of London, (1988) 285. https://books.google.com/books/about/The_Climate_of_London.html?hl=it&id=dsoO-3LF0GoC (accessed October 30, 2022).
[8] L. Mauri, G. Battista, E. de Lieto Vollaro, R. de Lieto Vollaro, Retroreflective materials for building's façades: Experimental characterization and numerical simulations, Sol. Energy 171 (2018) 150–156, https://doi.org/10.1016/J.SOLENER.2018.06.073.
[9] J. Yuan, C. Farnham, K. Emura, Performance of retro-reflective building envelope materials with fixed glass beads, Appl. Sci. 9 (2019) 1714, https://doi.org/10.3390/app9081714.
[10] K.M.A. Gabriel, W.R. Endlicher, Urban and rural mortality rates during heat waves in Berlin and Brandenburg, Germany, Environ. Pollut. 159 (8-9) (2011) 2044–2050.
[11] G. Battista, L. Evangelisti, C. Guattari, E. de Lieto Vollaro, R. de Lieto Vollaro, F. Asdrubali, Urban heat island mitigation strategies: experimental and numerical analysis of a University Campus in Rome (Italy), Sustainability 12 (2020) 7971, https://doi.org/10.3390/su12197971.
[12] X. Li, Y. Zhou, S. Yu, G. Jia, H. Li, W. Li, Urban heat island impacts on building energy consumption: A review of approaches and findings, Energy 174 (2019) 407–419, https://doi.org/10.1016/j.energy.2019.02.183.
[13] X. Yang, L.L.H. Peng, Z. Jiang, Y. Chen, L. Yao, Y. He, T. Xu, Impact of urban heat island on energy demand in buildings: Local climate zones in Nanjing, Appl. Energy 260 (2020), https://doi.org/10.1016/J.APENERGY.2019.114279.
[14] N. Kaloustian, D. Aouad, G. Battista, M. Zinzi, Leftover spaces for the mitigation of urban overheating in Municipal Beirut, Climate 6 (3) (2018) 68.
[15] M.A.D. Larsen, S. Petrović, A.M. Radoszynski, R. McKenna, O. Balyk, Climate change impacts on trends and extremes in future heating and cooling demands over Europe, Energ. Buildings 226 (2020), https://doi.org/10.1016/J.ENBUILD.2020.110397.
[16] Y. Abbassi, H. Ahmadikia, E. Baniasadi, Prediction of pollution dispersion under urban heat island circulation for different atmospheric stratification, Build. Environ. 168 (2020), https://doi.org/10.1016/j.buildenv.2019.106374.
[17] G. Battista, Analysis of the Air Pollution Sources in the city of Rome (Italy), Energy Procedia, Elsevier Ltd, 2017, pp. 392–397.
[18] Y. Du, C.M. Mak, Y. Li, A multi-stage optimization of pedestrian level wind environment and thermal comfort with lift-up design in ideal urban canyons, Sustain. Cities Soc. 46 (2019), https://doi.org/10.1016/J.SCS.2019.101424.
[19] S. Falasca, V. Ciancio, F. Salata, I. Golasi, F. Rosso, G. Curci, High albedo materials to counteract heat waves in cities: An assessment of meteorology, buildings energy needs and pedestrian thermal comfort, Build. Environ. 163 (2019), https://doi.org/10.1016/J.BUILDENV.2019.106242.
[20] J. Yang, S. Jin, X. Xiao, C. Jin, J. (Cecilia) Xia, X. Li, S. Wang, Local climate zone ventilation and urban land surface temperatures: Towards a performance-based and wind-sensitive planning proposal in megacities, Sustain Cities Soc. 47 (2019) 101487. https://doi.org/10.1016/J.SCS.2019.101487.
[21] H. Zhang, Z.-F. Qi, X.-Y. Ye, Y.-B. Cai, W.-C. Ma, M.-N. Chen, Analysis of land use/land cover change, population shift, and their effects on spatiotemporal patterns of urban heat islands in metropolitan Shanghai, China, Appl. Geogr. 44 (2013) 121–133.
[22] J. Mallick, A. Rahman, C.K. Singh, Modeling urban heat islands in heterogeneous land surface and its correlation with impervious surface area by using night-time ASTER satellite data in highly urbanizing city, Delhi-India, Adv. Space Res. 52 (2013) 639–655, https://doi.org/10.1016/J.ASR.2013.04.025.
[23] R.L. Hwang, C.Y. Lin, K.T. Huang, Spatial and temporal analysis of urban heat island and global warming on residential thermal comfort and cooling energy in Taiwan, Energ. Buildings 152 (2017) 804–812, https://doi.org/10.1016/J.ENBUILD.2016.11.016.
[24] H. Du, D. Wang, Y. Wang, X. Zhao, F. Qin, H. Jiang, Y. Cai, Influences of land cover types, meteorological conditions, anthropogenic heat and urban area on surface urban heat island in the Yangtze River Delta Urban Agglomeration, Sci. Total Environ. 571 (2016) 461–470, https://doi.org/10.1016/J.SCITOTENV.2016.07.012.
[25] C. Huang, T. Hu, Y. Duan, Q. Li, N. Chen, Q. Wang, M. Zhou, P. Rao, Effect of urban morphology on air pollution distribution in high-density urban blocks based on mobile monitoring and machine learning, Build. Environ. 219 (2022), https://doi.org/10.1016/J.BUILDENV.2022.109173.
[26] C. Mahaya, N. Zemmouri, H. Benharra, A. Elnokaly, Solar access assessment in semi-arid urban context: an application study for ten urban forms of existing apartment buildings districts in Batna City, Algeria, Sustain Cities Soc. 83 (2022), https://doi.org/10.1016/J.SCS.2022.103909.
[27] J. Younes, K. Ghali, N. Ghaddar, Diurnal selective radiative cooling impact in mitigating urban heat Island Effect, Sustain. Cities Soc. 83 (2022), https://doi.org/10.1016/J.SCS.2022.103932.
[28] S. Shareef, H. Altan, Urban block configuration and the impact on energy consumption: A case study of sinuous morphology, Renew. Sustain. Energy Rev. 163 (2022), https://doi.org/10.1016/J.RSER.2022.112507.
[29] A. Qaid, H. Bin Lamit, D.R. Ossen, R.N. Raja Shahminan, Urban heat island and thermal comfort conditions at micro-climate scale in a tropical planned city, Energ. Buildings 133 (2016) 577–595.

[30] M.B. Sosa, E.N. Correa, M.A. Cantón, Urban grid forms as a strategy for reducing heat island effects in arid cities, Sustain. Cities Soc. 32 (2017) 547–556, https://doi.org/10.1016/J.SCS.2017.05.003.
[31] H. Li, F. Meier, X. Lee, T. Chakraborty, J. Liu, M. Schaap, S. Sodoudi, Interaction between urban heat island and urban pollution island during summer in Berlin, Sci. Total Environ. 636 (2018) 818–828, https://doi.org/10.1016/J.SCITOTENV.2018.04.254.
[32] S. Parizotto, R. Lamberts, Investigation of green roof thermal performance in temperate climate: A case study of an experimental building in Florianópolis city, Southern Brazil, Energ. Buildings 43 (2011) 1712–1722, https://doi.org/10.1016/j.enbuild.2011.03.014.
[33] M.A. Bollman, G.E. DeSantis, R.S. Waschmann, P.M. Mayer, Effects of shading and composition on green roof media temperature and moisture, J. Environ. Manage. 281 (2021), https://doi.org/10.1016/j.jenvman.2020.111882.
[34] K.K. Roman, T. O'Brien, J.B. Alvey, O.J. Woo, Simulating the effects of cool roof and PCM (phase change materials) based roof to mitigate UHI (urban heat island) in prominent US cities, Energy 96 (2016) 103–117, https://doi.org/10.1016/j.energy.2015.11.082.
[35] E. Diz-Mellado, V.P. López-Cabeza, C. Rivera-Gómez, J. Roa-Fernández, C. Galán-Marín, Improving school transition spaces microclimate to make them liveable in warm climates, Appl. Sci. 10 (2020) 7648, https://doi.org/10.3390/app10217648.
[36] A. Aboelata, Vegetation in different street orientations of aspect ratio (H/W 1:1) to mitigate UHI and reduce buildings' energy in arid climate, Build. Environ. 172 (2020), https://doi.org/10.1016/j.buildenv.2020.106712.
[37] N.E. Theeuwes, A. Solcerová, G.J. Steeneveld, Modeling the influence of open water surfaces on the summertime temperature and thermal comfort in the city, J. Geophys. Res. Atmos. 118 (2013) 8881–8896, https://doi.org/10.1002/jgrd.50704.
[38] J. Fahed, E. Kinab, S. Ginestet, L. Adolphe, Impact of urban heat island mitigation measures on microclimate and pedestrian comfort in a dense urban district of Lebanon, Sustain. Cities Soc. 61 (2020), https://doi.org/10.1016/j.scs.2020.102375.
[39] G. Battista, E. de Lieto Vollaro, S. Grignaffini, P. Ocłoń, A. Vallati, Experimental investigation about the adoption of high reflectance materials on the envelope cladding on a scaled street canyon, Energy. 230 (2021) 120801. https://doi.org/10.1016/j.energy.2021.120801.
[40] A.D.L. Vollaro, G. Galli, A. Vallati, R. Romagnoli, Analysis of thermal field within an urban canyon with variable thermophysical characteristics of the building's walls, J. Phys. Conf. Ser. 655 (2015) 012056.
[41] M. Matias, A. Lopes, Surface radiation balance of urban materials and their impact on air temperature of an urban canyon in Lisbon, Portugal, Appl. Sci. 10 (2020) 2193, https://doi.org/10.3390/app10062193.
[42] C. Georgakis, S. Zoras, M. Santamouris, Studying the effect of "cool" coatings in street urban canyons and its potential as a heat island mitigation technique, Sustain. Cities Soc. 13 (2014) 20–31, https://doi.org/10.1016/J.SCS.2014.04.002.
[43] F. Peron, M.M. de Maria, F. Spinazzè, U. Mazzali, An analysis of the urban heat island of Venice mainland, Sustain. Cities Soc. 19 (2015) 300–309, https://doi.org/10.1016/J.SCS.2015.05.008.
[44] J. Wang, Q. Meng, K. Tan, L. Zhang, Y. Zhang, Experimental investigation on the influence of evaporative cooling of permeable pavements on outdoor thermal environment, Build. Environ. 140 (2018) 184–193, https://doi.org/10.1016/J.BUILDENV.2018.05.033.
[45] X.D. Xiao, L. Dong, H. Yan, N. Yang, Y. Xiong, The influence of the spatial characteristics of urban green space on the urban heat island effect in Suzhou Industrial Park, Sustain. Cities Soc. 40 (2018) 428–439, https://doi.org/10.1016/J.SCS.2018.04.002.
[46] G. Battista, E.M. Pastore, L. Mauri, C. Basilicata, Green roof effects in a case study of Rome (Italy), Energy Procedia 101 (2016) 1058–1063.
[47] M. Zinzi, S. Agnoli, C. Burattini, B. Mattoni, On the thermal response of buildings under the synergic effect of heat waves and urban heat island, Sol. Energy 211 (2020) 1270–1282, https://doi.org/10.1016/J.SOLENER.2020.10.050.
[48] M. Zinzi, E. Carnielo, B. Mattoni, On the relation between urban climate and energy performance of buildings. A three-years experience in Rome, Italy, Appl. Energy. 221 (2018) 148–160, https://doi.org/10.1016/J.APENERGY.2018.03.192.
[49] G. Battista, R. de Lieto Vollaro, M. Zinzi, Assessment of urban overheating mitigation strategies in a square in Rome, Italy, Sol. Energy 180 (2019) 608–621, https://doi.org/10.1016/j.solener.2019.01.074.
[50] F. Salata, I. Golasi, R. de Lieto Vollaro, A., de Lieto Vollaro, Outdoor thermal comfort in the Mediterranean area. A transversal study in Rome, Italy, Build. Environ. 96 (2016) 46–61, https://doi.org/10.1016/J.BUILDENV.2015.11.023.
[51] G. Battista, E. Carnielo, R. De Lieto Vollaro, Thermal impact of a redeveloped area on localized urban microclimate: A case study in Rome, Energ. Buildings 133 (2016) 446–454.
[52] F. Salata, I. Golasi, D. Petitti, E. de Lieto Vollaro, M. Coppi, A. de Lieto Vollaro, Relating microclimate, human thermal comfort and health during heat waves: An analysis of heat island mitigation strategies through a case study in an urban outdoor environment, Sustain. Cities Soc. 30 (2017) 79–96, https://doi.org/10.1016/J.SCS.2017.01.006.
[53] G. Battista, E.M. Pastore, Using cool pavements to mitigate urban temperatures in a case study of Rome (Italy), Energy Procedia 113 (2017) 98–103.
[54] V. Costanzo, G. Evola, L. Marletta, Energy savings in buildings or UHI mitigation? Comparison between green roofs and cool roofs, Energy Build. 114 (2016) 247–255, https://doi.org/10.1016/J.ENBUILD.2015.04.053.
[55] F. Marando, E. Salvatori, A. Sebastiani, L. Fusaro, F. Manes, Regulating Ecosystem Services and Green Infrastructure: assessment of Urban Heat Island effect mitigation in the municipality of Rome, Italy, Ecol. Model. 392 (2019) 92–102, https://doi.org/10.1016/J.ECOLMODEL.2018.11.011.
[56] E. Di Giuseppe, M. Pergolini, F. Stazi, Numerical assessment of the impact of roof reflectivity and building envelope thermal transmittance on the UHI effect, Energy Procedia 134 (2017) 404–413, https://doi.org/10.1016/J.EGYPRO.2017.09.590.
[57] A. Salvati, P. Monti, H. Coch Roura, C. Cecere, Climatic performance of urban textures: Analysis tools for a Mediterranean urban context, Energ. Buildings 185 (2019) 162–179, https://doi.org/10.1016/J.ENBUILD.2018.12.024.
[58] ENVI-met - Decode urban nature with Microclimate simulations, (n.d.). https://www.envi-met.com/it/ (accessed October 30, 2022).
[59] Roma2Pass, (n.d.). https://www.roma2pass.it/ (accessed January 12, 2023).
[60] G. Battista, L. Evangelisti, C. Guattari, M. Roncone, C.A. Balaras, Space-time estimation of the urban heat island in Rome (Italy): Overall assessment and effects on the energy performance of buildings, Build. Environ. 228 (2023), https://doi.org/10.1016/J.BUILDENV.2022.109878.
[61] E. Cacciari, S. Milani, A. Balsamo, E. Spada, G. Bona, L. Cavallo, F. Cerutti, L. Gargantini, N. Greggio, G. Tonini, A. Cicognani, Italian cross-sectional growth charts for height, weight and BMI (2 to 20 yr), J. Endocrinol. Invest. 29 (2006) 581–593, https://doi.org/10.1007/BF03344156/METRICS.
[62] P. Grasgruber, J. Cacek, T. Kalina, M. Sebera, The role of nutrition and genetics as key determinants of the positive height trend, Econ. Hum. Biol. 15 (2014) 81–100, https://doi.org/10.1016/J.EHB.2014.07.002.